HIGH-DENSITY DIFFUSE OPTICAL TOMOGRAPHY AND FINITE ELEMENT MODELS

UDK 004.92:519.6:543.4

GUCHEK Petro
Dr.Sc., Associate Professor at the Department of information technologies, Kherson National Technical University; Institute of biocybernetics and biomedical engineering of M. Nalecha of the Polish academy of Sciences (Poland).
Scientific interests: information technologies, mathematical modeling, scientific visualization

OLENA Litvinenko
PhD., Associate Professor at the Department of higher mathematics and mathematical modeling, Kherson National Technical University.
Scientific interests: mathematical modeling, information technologies, methods and models recovery of functions

IGOR Astionenko
PhD., Associate Professor at the Department of higher mathematics and mathematical modeling, Kherson National Technical University.
Scientific interests: mathematical modeling, information technologies, methods and models recovery of functions

ABSTRACT

Optical spectroscopy methods are widely used in medical practice for diagnostic purposes in various diseases. The internal biomechanical responses of the brain cannot be completely measured by experimental techniques. Analytical models are limited to problems with regular geometry, simple boundary conditions and homogeneous material properties. Numerical approaches, on the other hand, approximate the analytical solution with a numerical procedure. For deep research and visualization of ongoing processes, many software systems use the finite element method. Geometrically complex material domains of the problem can be represented by a collection of geometrically simple sub domains called Finite Elements. This paper outlines new models of the serendipity finite element family for the simulation of the light propagation in biological tissue of the human head.

Introduction

At present, optical spectroscopy methods are widely used in medical practice for diagnostic purposes and occupy one of the leading positions next to X-ray, acoustic, nuclear magnetic resonance, radionuclide, endoscopic, etc.

Light visible in near infrared wavelength range is safe at low levels of emission density, the human body is well adapted to this type of emission. Light of this wavelength range penetrates well into biological tissue, interacts with various structural and dynamic components of tissues and carries information about the structural and dynamic changes occurring in tissues in various diseases. Such well-known phenomena in physics as absorption, diffraction, interference, fluorescence, as well as elastic, quasi-elastic and molecular scattering, are observed in biological media and are sources of information about pathological processes[1].

Transparency of biological tissues reaches its maximum in the near infrared (NIR), which is due to the fact that living tissues do not contain strong internal chromophores that absorb emission in this region of the spectrum. Light penetrates into tissues to a depth of several centimeters, which is important for the transmission of voluminous human organs. However, biological tissues are characterize by the sufficiently strong scattering of NIR emission, which prevents clear images of local inhomogeneities arising from various pathologies, such as the formation of tumors or local growth of blood volume due to hemorrhage or overgrowth of microvessels[2-4].

Significant perspectives, from the point of view of safety, simplicity and reliability of devices, as well as obtaining

reliable information about physiological processes, have optical diffusion tomography [6,7] and optical coherence tomography [5].

One of the most common software package with open-source is Near Infrared Fluorescence and Spectral Tomography (NIRFAST), which simulates light propagation in biological tissue based on the finite element method (FEM). In biomechanical studies, Finite Element (FE) customized meshes start to be more and more interesting since they can integrate both geometry and mechanical properties of the patient.

This paper outlines new models of the serendipity finite element family for the simulation of the light propagation in biological tissue of the human head.

LITERATURE SURVEY

NIR techniques in biomedical sciences are based on two important physical observations: (1) Light in the NIR range is weakly absorbed by tissue and thus it can penetrate several centimeters through tissue and be detected by sensors; (2) Different forms of hemoglobin, oxygenated and deoxygenated, arc the main chromophores of living tissue in the NIR wavelength range, and have distinct absorption spectra[9]. The former presents the feasibility of NIR detection in biological tissue, while the latter lays the foundation of NIR measurement to provide enough anatomic and functional contrast between soft tissues and directly monitors the hemoglobin changes. Any physiological phenomenon or disease, such as brain activity, cancer, hemotoma, etc., which causes differences in the oxygen content or the hemoglobin concentration in normal tissue, can in principle be diagnosed by the NIR diffuse optical method with simultaneous measurements made at two or more NIR wavelengths. Scattering is the dominant interaction mechanism of NIR light with biological tissue and helps distinguish between tissues, although the associated physiological information is still being researched [1,5,6,7].

Light propagates in biological tissue, depending on the combination of absorption, scattering and reflection properties of photons. The absorption and scattering of photons depend on the wavelength. Dispersion decreases with increasing wavelength and at the same time facilitates the transmission of near-infrared light photons over long distances compared to visible light. Reflection also depends on the angle of the light beam, as well as the surface of the tissue [9].

When the absorption of a light beam takes place, its energy is dissipated as thermal energy throughout the absorber [9,10]. At certain wavelengths, is absorption occurs, determined by the molecular properties of materials on the light path [8].

The basic light-absorbing compounds in biological tissue within the near-infrared range are called chromophores [9]. Most chromophores can be considered to have stable concentrations during a measurement period (~10 min), however, there presence adds to the total light attenuation (i.e. melanin, bilirubin, water). The primary chromophores of interest are oxyhemoglobin (HbO2), deoxyhemoglobin (Hb) and cytochrome c oxidase, because the concentration of these chromophores varies with time and oxygenation status [8].

In this regard, when monitoring oxygenation of tissues with NIRS, the chromophores Hb and HbO2 are of interest. Hb and HbO2 are responsible for the delivery, transportation and removal of oxygen (O2) and carbon dioxide (CO2) throughout the human body. For enlightenment of brain and muscle tissues.

NIRS devices use light in the wavelength range 700-1000 nm. This range follows from increased H2O absorption bands above 1000 nm and increased scattering and more intense absorption bands of Hb below 700 nm. In the 700-1000 nm range, Hb and HbO2 possess unique absorption spectra, which allows the emitted light to propagate through the tissue a few centimeters [11].

From the optical point of view, the human head can be viewed as an inhomogeneous layered structure that consists of a layer of dermis (scalp), a layer of bone (skull), irregular and relatively thin layer of cerebrospinal fluid (CSF), a layer of gray matter and, finally, a deep region of white matter [12].The diffusion of light strongly depends on this heterogeneity. In particular, CSF has been the subject of many studies because of its "light directing" effect, depending on its transparency [13] and its reticular structure consisting of arachnoids that can strongly affect light scattering [14-16].

A strong knowledge of the optical properties (namely the reduced scattering coefficient and the absorption coefficient) of head structures is undoubtedly fundamental, not only for the technical optimization of these techniques, but

also for a deeper understanding of their potential. For example, the assessment of main parameters like the volume probed by light, the light penetration depth and also the mean optical path length can be made if a prior information of both anatomical and optical parameters is available [17].

In addition, knowledge of optical properties over a wide spectral range provides additional information about the tissue: the scattering spectrum is related to the structure and absorption spectrum of the composition [18].

In literature there are studies reporting on ex-vivo or post-mortem measurements for the characterization of the human head optical properties, [19–24] but they are not representative of an in-vivo condition.

In some studies, optical properties are considered in vivo [25-27], but the data presented are preliminary or limited to several subjects or obtained after approximations (for example, the head was modeled as a homogeneous medium). In addition, comparative analysis with a different methodology is not presented.

In the finite element method an important role plays the finite element serendipity family [28]. Finite elements of serendipity family are a useful class of discrete models. For the first time these elements were obtained in 1968 with the help of resourceful recruiting because they did not lend any formalization. Finite elements of serendipity family are the result of modification of finite element Lagrangian families by eliminating internal nodes.

For building functions of the form a finite element traditionally used matrix process [28]. Method a systematic generation functions of the form, proposed by Taylor in 1972, led to the known standard models on the elements serendipity family [29]. In the 70s of the last century through the work Uachspressa the method of the "product of planes" to construct basic functions FE [30]. But this method has not been applied to serendipity finite elements (SFE). In the early 80's was offered a probability-geometric method of constructing bases of finite elements of different configurations [31]. The advantages of this method are most clearly manifested in serendipity models. For construction of serendipity elements used geometric method [32]. This modification method "product of planes", which uses the technique of multiplication equations of planes and surfaces of second order. New methods greatly simplify the process of building functions of the form (there is no need to solve a system of linear equations corresponding order on the item) and allow for alternative models SFE. The presence of "outside of the nodal" parameters in models obtained using the new method makes it possible to get rid of the shortcomings that are inherent in the standard model (eg, negative values of loads in the nodes).

However construction of the basic functions of these methods makes it impossible to build the function form with predetermined characteristics. To solve the problem of interpolation SFE in [33] proposed a method of constructing an analytical hierarchical forms the basis functions [34].

METHODS

From the instrumentation point of view, NIRS, DOT and OT are categorized according to the source-detector (referred to as optode) installation. The past two decades have witnessed significant progress in the NIR diffuse optical method starting with the development of three main irradiation-measurement schemes that use continuous wave (CW), frequency domain (FD) and time domain or time-resolved (TR) techniques respectively. Of these schemes, it is generally believed and numerically demonstrated that a TR system can provide the most information on local distributions of optical properties in tissue, at the expense of increased system complexity, longer data acquisition time and higher cost. In recent years, much effort has been devoted by an increasing number of relevant laboratories, to developing the compact, low noise and high photon counting rate TR systems.

A NIRS device consists out of a light source (emitting optode) to deliver light to the tissues and a light detector (receiving optode), which measures the intensity of the exiting light. A computer translates the change in light intensity to clinically useful information. The receiving optode can be either contralateral (transmission NIRS) or ipsilateral (reflectance-mode NIRS) located at the receiver, see Fig. 1A and B. Transmission cerebral NIRS, in which a near-infrared light source is placed contralateral to the receiver, is most frequently used in infants. In adults this is not believed to be sensitive enough, primarily because of the reduced intensity of the exiting near-infrared light[9] and poor signal-to-noise ratio [36]. In reflectance-mode NIRS the near-infrared light source is placed ipsilateral to the receiver, it has been developed to overcome the problems of transmission NIRS. This approach assumes that

there is a homogeneous light absorption and constant optical scattering effects. If these assumptions are correct, then the mean pathlength of the travelling photons should describe an ellipse whose mean depth is proportional (i.e. 1/3) to the optode spacing [36-37]. In Fig. 2C a NIRS device that uses two receiving optodes is displayed. This device attempts to differentiate between light attenuation caused by skull and overlying tissues and light attenuation caused by cerebral tissue. This is called the multi-distance approach and is used in several types of spectrometer, such as spatially resolved spectroscopy and functional NIRS. In most of the NIRS instruments, the distance between source and detector on the surface of the tissue varies between 3 and 5 cm. Measurements at larger distances are difficult because of the fast decay of the signals with the inter-optode distance [11,48].

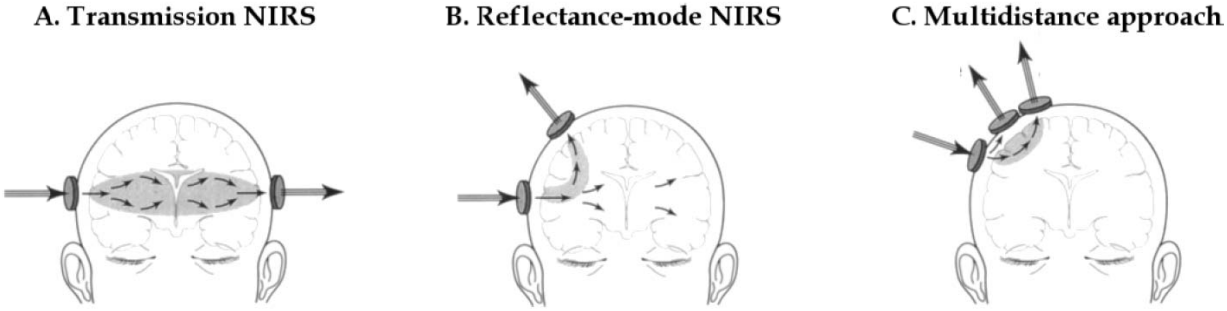

Fig. 1. Different type of NIRS set-ups: (a) transmission NIRS, (b) reflectance-mode NIRS, (c) multi-distance approach NIRS with several receiving optodes to differ between oxygenation changes in different tissue layers [35].

Before the NIR light reaches the brain it must first pass through the different tissue layers, see Fig. 2. In some of these layers there are chromophores present, which will cause light attenuation independent of brain oxygenation.

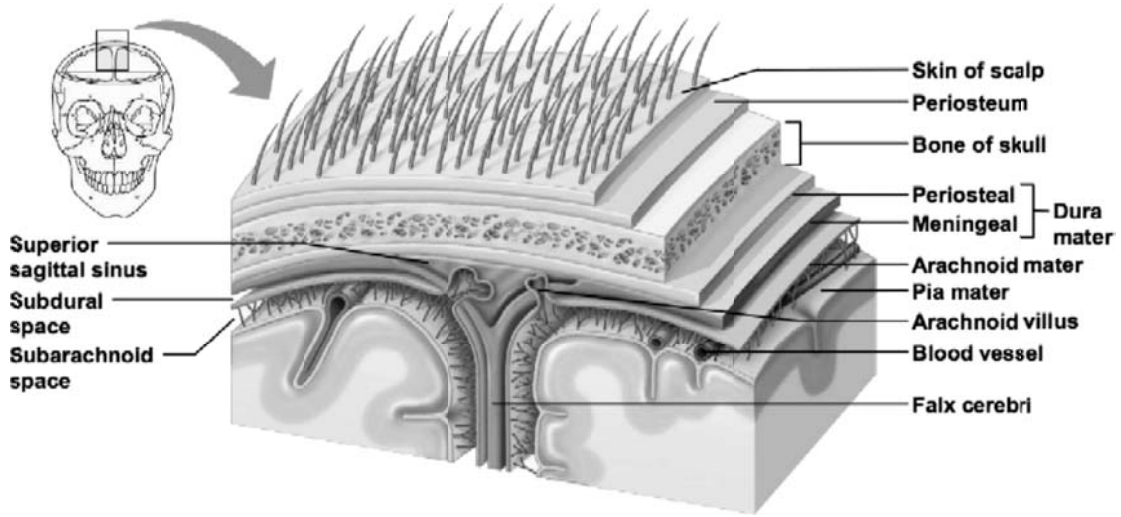

Fig. 2. Different tissue layers of the human head [38,48].

The skin is composed of the epidermis and the dermis. The epidermis contains melanin, at near-infrared wavelengths melanin has a constant specific extinction coefficient and it also has a significant optical effect on skin reflectance. For example, Caucasian skin causes two times more reflection than Negroid skin in the 600-1000 nm region. Since its absorption is constant and oxygenation independent, it does not produce attenuation changes that are time dependent[39].

The dermis and the skull contain the chromophores bilirubin, hemoglobin and cytochrome c oxidase. Overall, the skin and the skull provide a barrier which must be penetrated before light enters the brain tissues. The attenuation caused by this region will also change with oxygenation

(due to the presence of hemoglobin), the magnitude of this effect is proportional to its thickness and chromophore concentration. Therefore it is recommended that the thickness of brain tissue illuminated is much greater than that of the surface tissues[48].

In the brain water and lipids are present together with bilirubin, hemoglobin, and cytochrome c oxidase. The average water content of neonatal brain is 90% [42] and 80% [43] for an adult brain. This obviously implies that any absorption band of water will have a large optical effect. An infant's brain consists of about 80% of water, lipids constitute about 5% of the total wet weight. This percentage increases to 8% of the grey matter and 17% of the white matter in adulthood [42].

There are several factors influencing the optical pathlength including tissue type, wavelength, scattering coefficients, optode geometry and blood volume changes. In reality there is no unique optical path through a scattering medium but rather a distribution of paths[39,48].

The internal biomechanical responses of the brain cannot be completely measured by experimental techniques. Analytical models are limited to problems with regular geometry, simple boundary conditions and homogeneous material properties. Numerical approaches, on the other hand, approximate the analytical solution with a numerical procedure. The FEM is superior to other numerical methods. Geometrically complex material domains of the problem can be represented by a collection of geometrically simple sub domains called Finite Elements. The approximation functions are then derived over each finite element, since any continuous function can be represented by a linear combination of algebraic polynomials. This can be viewed as a piece wise application of the variational methods, in which the approximation functions are algebraic polynomials.

Finite element models are repeatable and reproducible, and simulations can be seen as surrogate experiments without biological variability. They can also include irregular geometry, inhomogeneous and nonlinear material properties and complex boundary.

In the biomechanical field, numerical techniques were first used to complement experimental car crash simulations. Today, the numerical technique has reached such a level that complex structures like the human being can be modeled with good accuracy. However, much research remains to be done before a complete model of the human being can be presented.

The initial step in developing 3 dimensional finite element model of the human head is to obtain some set of MRI scanned images of human head. After the Preprocessing of the image data, the set of images are imported to software and using suitable developed algorithm the 3Dimensional meshed finite element model can be obtained. The important parameters which affect the FEM model of the human head is mesh method and mesh quality, see Fig. 3.

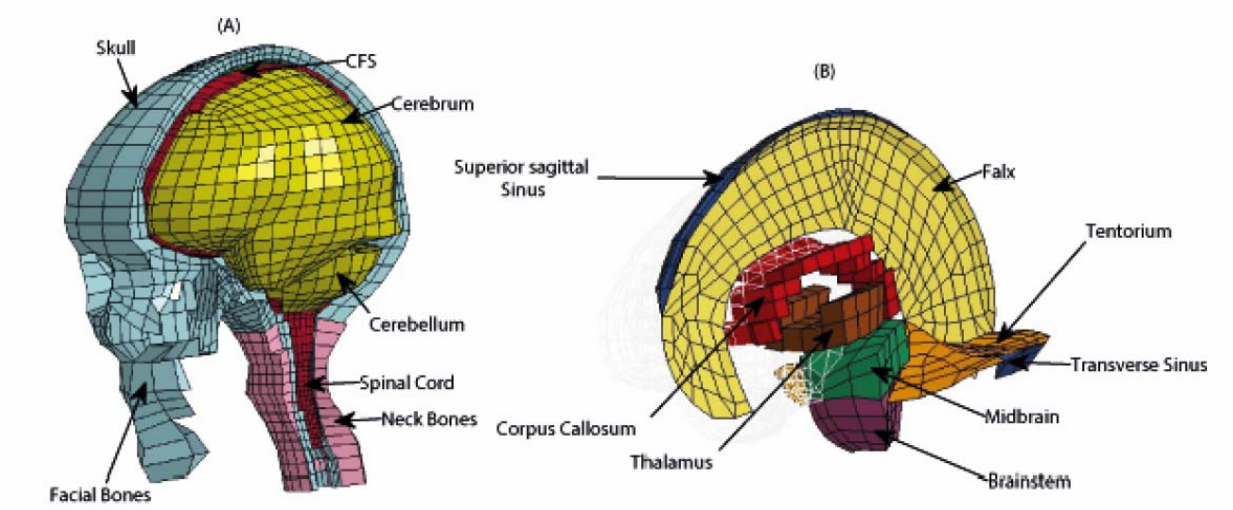

Fig.3. Finite element model of the human head. (A) isometric view of the head model with brain exposed; (B) internal view of the head model. [44]

Using matrix methods to serendipity elements have shape functions called standard. Matrix method was developed in the works of Vandermonde, Cauchy, Lagrange interpolation problems concerning functions of one argument. In the FEM it is considered the main method of constructing polynomial interpolation for functions of two or three arguments. For example, the process of building a basis for FE with 4 nodes (Fig. 4) begins with the choice of 4-parametric polynomial with two arguments:

$$\varphi(\xi,\eta)=\alpha_1+\alpha_2\xi+\alpha_3\eta+\alpha_4\xi\eta \text{ , де } \begin{matrix}|\xi|\le 1,\\ |\eta|\le 1\end{matrix} \quad (1)$$

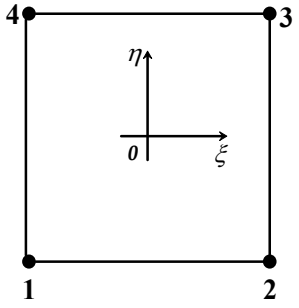

Fig.4. The element with bilinear basis (FE-4)

The functions form bilinear interpolation $N_i(\xi,\eta)$ $(i=1,2,3,4)$ which must satisfy the interpolation hypothesis

$$N_i(\xi_k,\eta_k)=\delta_{ik}\ ,\quad i,k=\overline{1,4}\ , \quad (2)$$

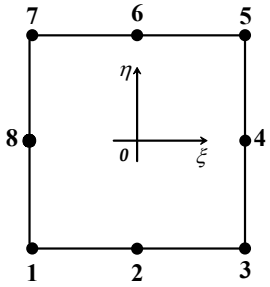

Fig.5. SFE-8
$(|\xi|\le 1\ ,|\eta|\le 1)$

Using an analytical method for constructing hierarchical forms the basis functions, the set of basis functions SFE-8 may be obtained by adding to the surface of a standard basis [34]:

$$N_1^{(S)}(\xi,\eta)=\frac{1}{4}(1-\xi)(1-\eta)(-1-\xi-\eta), \quad (6)$$

where δ_{ik} – is the Kronecker delta, *i* – is the number of functions and *k* – is the number of nodes.

Using (2) leads to a system of linear algebraic equations 4×4 with relative parameters α_j :

$$\alpha_1+\alpha_2\xi_k+\alpha_3\eta_k+\alpha_4\xi_k\eta_k=\delta_{ik}\ . \quad (3)$$

Find the unknown parameters α_j and write the interpolation polynomial (1) in the form [28]:

$$\varphi(\xi,\eta)=N_1(\xi,\eta)\Phi_1+N_2(\xi,\eta)\Phi_2+N_3(\xi,\eta)\Phi_3+N_4(\xi,\eta)\Phi_4=[N_i]\{\Phi_i\}, \quad (4)$$

where $[N_i]$ – matrix-row basis functions FE ($i=1,2,3,4$); $\{\Phi_i\}$ – matrix-column boundary values function that interpolates.

We get bilinear basis functions for the FE-4:

$$N_i=\frac{1}{4}(1+\xi_i\xi)(1+\eta_i\eta)\ ,\quad i=1,2,3,4\ ; \quad (5)$$
$$\xi_i,\eta_i=\pm1\ .$$

The functions of the form (basic functions) $N_i(\xi,\eta)$ play an important role in the finite element method - approximate field in the middle of the element. The choice of approximating functions and their properties is largely dependent on the accuracy of the solution. It was important to note that serendipity model is a unique example of simultaneous interpolation and approximation - they interpolate function on the boundary element and approximate inside it.

We will consider finite elements serendipity family biquadratic and bicubic interpolation (Fig. 5, Fig. 6) [28,45].

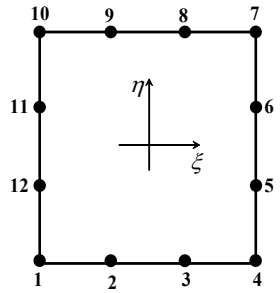

Fig.6. SFE-12
$(|\xi|\le 1\ ,|\eta|\le 1)$

$$N_2^{(S)}=\frac{1}{2}(1-\xi^2)(1-\eta) \quad (7)$$

hyperbolic paraboloid with coefficient K :

$$N_1=\frac{1}{4}(1-\xi)(1-\eta)(-1-\xi-\eta+K(1+\xi)(1+\eta)), \quad (8)$$

$$N_2 = \frac{1}{2}(1-\xi)(1-\eta)\left((1+\xi)-\frac{1}{2}K(1+\xi)(1+\eta)\right), \quad (9)$$

where $N_1^{(S)}, N_2^{(S)}$ - standard basis functions SFE-8,

N_1, N_2 - modified basis functions SFE-8.

Now we get generalized formula for building alternative basis functions biquadratic elements:

$$N_i = \frac{1}{4}(1+\xi_i\xi)(1+\eta_i\eta)(-1+\xi_i\xi+\eta_i\eta+K(1-\xi_i\xi)(1-\eta_i\eta)), \quad (10)$$
$$i = 1,3,5,7; \quad \xi_i = \pm 1; \quad \eta_i = \pm 1.$$

$$N_i = \frac{1}{2}(1-\xi)(1+\eta_i\eta)\left((1+\xi)-\frac{1}{2}K(1+\xi)(1-\eta_i\eta)\right) \quad (11)$$
$$, \quad i = 2,6; \quad \eta_i = \pm 1.$$

$$N_i = \frac{1}{2}(1-\eta)(1+\xi_i\xi)\left((1+\eta)-\frac{1}{2}K(1+\eta)(1-\xi_i\xi)\right) \quad (12)$$
$$, \quad i = 4,8; \quad \xi_i = \pm 1.$$

Similarly, using the analytical method for constructing hierarchical forms the basis functions receive a multiplicity of basis functions SFE-12 added to the surface of a standard basis [34]:

$$N_1^{(S)} = \frac{1}{32}(1-\xi)(1-\eta)(9\xi^2+9\eta^2-10), \quad (13)$$

$$N_2^{(S)} = \frac{9}{32}(1-\xi^2)(1-\eta)(1-9\xi), \quad (14)$$

hyperbolic paraboloid with coefficient K:

$$N_1 = \frac{1}{4}(1-\xi)(1-\eta)\left(\frac{1}{8}(9\xi^2+9\eta^2-10)+K\cdot\frac{9}{4}\cdot(1+\xi)(1+\eta)\right), \quad (15)$$

$$N_2 = \frac{3}{8}(1-\xi)(1-\eta)\left(\frac{3}{4}(1+\xi)(1-3\xi)-K\cdot\frac{3}{4}\cdot(1+\xi)(1+\eta)\right), \quad (16)$$

where $N_1^{(S)}, N_2^{(S)}$ - standard basis functions SFE-12,

N_1, N_2 - modified basis functions SFE-12.

Now we write generalized formula for building alternative basis functions bicubic elements:

$$N_i = \frac{1}{4}(1+\xi_i\xi)(1+\eta_i\eta)\times$$
$$\times\left(\frac{1}{8}(9\xi^2+9\eta^2-10)+K\cdot\frac{9}{4}\cdot(1-\xi_i\xi)(1-\eta_i\eta)\right), \quad (17)$$
$$i = 1,4,7,10; \quad \xi_i, \eta_i = \pm 1;$$

$$N_i = \frac{3}{8}(1+3\xi_i\xi)(1+\eta_i\eta)\times$$
$$\times\left(\frac{3}{4}(1-3\xi_i\xi)(1+9\xi_i\xi)-K\cdot\frac{3}{4}(1-3\xi_i\xi)(1-\eta_i\eta)\right), \quad (18)$$

$$i = 2,3,8,9, \quad \eta_i = \pm 1, \quad \xi_i = \pm\frac{1}{3}.$$

$$N_i = \frac{3}{8}(1+3\eta_i\eta)(1+\xi_i\xi)\times$$
$$\times\left(\frac{3}{4}(1-3\eta_i\eta)(1+9\eta_i\eta)-K\cdot\frac{3}{4}(1-3\eta_i\eta)(1-\xi_i\xi)\right), \quad (19)$$

$$i = 5,6,11,12, \quad \xi_i = \pm 1, \quad \eta_i = \pm\frac{1}{3}.$$

The resulting basis functions meet all the qualities that are inherent for basis functions form the SFE [28,34].

New analytical method for constructing hierarchical forms of basis functions can be easily extended and to three-dimensional finite elements (Fig. 7, Fig. 8).

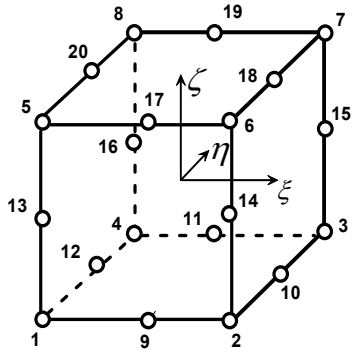

Fig.7. SFE-20

$(|\xi| \le 1, |\eta| \le 1, |\zeta| \le 1)$

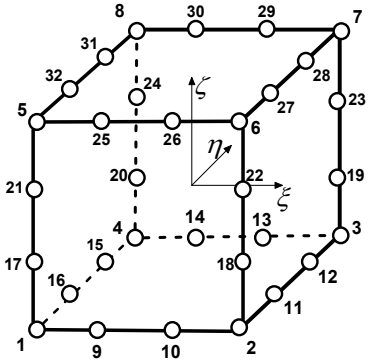

Fig.8. SFE-32

$(|\xi| \le 1, |\eta| \le 1, |\zeta| \le 1)$

For element SFE-20 from the literature [28,46] only one basis is known. Basic functions for 1 and 9 nods recorded in the formulas:

$$N_1(\xi,\eta,\zeta)=\frac{1}{8}(1-\xi)(1-\eta)(1-\zeta)(-\xi-\eta-\zeta-2), \tag{20}$$

$$N_9(\xi,\eta,\zeta)=\frac{1}{4}(1-\xi^2)(1-\eta)(1-\zeta). \tag{21}$$

The set of alternative basis functions may be obtained by combining the standard basis functions (formulas (20), (21)) with of the surface of the second order with the corresponding coefficient K :

$$N_1=\frac{1}{8}(1-\xi)(1-\eta)(1-\zeta)\times \\ \times\left((-2-\xi-\eta-\zeta)+K(\xi\eta+\xi\zeta+\eta\zeta+2\xi+2\eta+2\zeta+3)\right), \tag{22}$$

$$N_9=\frac{1}{4}(1-\xi)(1-\eta)(1-\zeta)\left((1+\xi)-\frac{1}{2}K(1+\xi)(2+\eta+\zeta)\right). \tag{23}$$

Now we get generalized formula for building alternative basis functions SFE-20:

$$N_i=\frac{1}{8}(1+\xi_i\xi)(1+\eta_i\eta)(1+\zeta_i\zeta)\times(-2+\xi_i\xi+\eta_i\eta+\zeta_i\zeta+ \\ +K(\xi_i\eta_i\xi\eta+\xi_i\zeta_i\xi\zeta+\eta_i\zeta_i\eta\zeta-2\xi_i\xi-2\eta_i\eta-2\zeta_i\zeta+3)), \\ \xi_i,\eta_i,\zeta_i=\pm1,\quad i=\overline{1,8}, \tag{24}$$

$$N_i=\frac{1}{4}(1-\xi^2)(1+\eta_i\eta)(1+\zeta_i\zeta)\left(1-\frac{1}{2}K(2-\eta_i\eta-\zeta_i\zeta)\right), \\ \eta_i,\zeta_i=\pm1,\ \text{i}=9,11,17,19. \tag{25}$$

Other functions we get from (25) by cyclic rearrangement ξ,η,ζ .

Similarly, we show the analytical method for constructing hierarchical forms basis functions on three-dimensional element, which contains 32 nods with tricubic interpolation [47].

For element SFE-32 from the literature [46] also only one basis is known. Basic functions for 1 and 9 nods recorded in the formulas:

$$N_1(\xi,\eta,\zeta)=\frac{1}{64}(1-\xi)(1-\eta)(1-\zeta)\left(9(\xi^2+\eta^2+\zeta^2)-19\right), \tag{26}$$

$$N_9(\xi,\eta,\zeta)=\frac{9}{64}(1-\xi^2)(1-3\xi)(1-\eta)(1-\zeta). \tag{27}$$

The set of alternative basis functions may be obtained by combining the standard basis functions (formulas (26), (27)) with of the surface of the second order with the corresponding coefficient K :

$$N_1=\frac{1}{8}(1-\xi)(1-\eta)(1-\zeta)\times \\ \left(\frac{1}{8}(9(\xi^2+\eta^2+\zeta^2)-19)+\frac{9}{4}K(\xi\eta+\eta\zeta+\xi\zeta+2(\xi+\eta+\zeta)+3)\right) \tag{28}$$

$$N_9=\frac{3}{16}(1-\xi)(1-\eta)(1-\zeta)\times \\ \times\left(\frac{3}{4}(1+\xi)(1-3\xi)-\frac{3}{4}K(1+\xi)(2+\eta+\zeta)\right). \tag{29}$$

Now we get generalized formula for building alternative basis functions SFE-32:

$$N_i = \frac{1}{8}(1+\xi_i\xi)(1+\eta_i\eta)(1+\zeta_i\zeta)\times(\frac{1}{8}(9\xi^2+9\eta^2+9\zeta^2-19)+$$
$$+\frac{9}{4}K(\xi_i\eta_i\xi\eta+\eta_i\zeta_i\eta\zeta+\xi_i\zeta_i\xi\zeta-2\xi_i\xi-2\eta_i\eta-2\zeta_i\zeta+3)), \quad (30)$$
$$\xi_i,\eta_i,\zeta_i=\pm1, \quad i=\overline{1,8};$$

$$N_i = \frac{3}{16}(1-\xi^2)(1+\eta_i\eta)(1+\zeta_i\zeta)\times$$
$$\times\left(\frac{3}{4}(1+9\xi_i\xi)-\frac{3}{4}K(2-\eta_i\eta-\zeta_i\zeta)\right), \quad (31)$$
$$\xi_i=\pm\frac{1}{3}, \ \eta_i,\zeta_i=\pm1, \ \text{i}=9,10,13,14,25,26,29,30.$$

Other functions we get from (31) by cyclic rearrangement ξ,η,ζ .

CONCLUSIONS

In biomedical studies, Finite Elements have been more and more interesting since they can integrate both geometry and mechanical properties of the patient. This paper, we consider new mathematical models of serendipity finite elements obtained by the analytical method of constructing hierarchical forms of basis functions. A promising point for further studies is the application of these models in solving problems of modeling the propagation of light in the biological tissue of the human head. And also the comparative analysis with existing models and revealing of those which have the best computational properties.

REFERENCES:

1. Tuchin V.V. Handbook of optical biomedical diagnostics / V.V. Tuchin. – Belingham, Washington. – 2002. – 1093 p.
2. Muller G. Medical Optical Tomography: Functional Imaging and Monitoring / Ed. by G. Muller, B. Chance, R. Alfano. – et al. Bellingham, WA: SPIE Press, 1993. – V. IS11.
3. Tuchin V.V. Selected Papers on Tissue Optics: Applications in Medical Diagnostics and Therapy / Ed. by V. V. Tuchin. – Bellingham, WA: SPIE Press, 1994. V. MS102.
4. Chance B. Phase measurement of light absorption and scatter in human tissue / B. Chance, M. Cope, E.Gratton , N. Ramanujam , B.Tromberg. – Rev. Sci. Instrum. 1998. V. 69, №10. P. 3457-3481.
5. Drexler W. Optical Coherence Tomography: Technology and Applications / Ed. by W. Drexler, J. G. Fujimoto. – Berlin: Springer, 2008.
6. Sawosz P. "Experimental estimation of the photons visiting probability profiles in time-resolved diffuse reflectance measurement"/ P. Sawosz, M. Kacprzak, W. Weigl, A. Borowska-Solonynko, P. Krajewski, N. Zolek, B. Ciszek, R. // Phys. Med. Biol. – 2012 – 57(23). – 7973–7981.
7. Liebert A. "Time-resolved multidistance near-infrared spectroscopy of the adult head: intracerebral and extracerebral absorption changes from moments of distribution of times of flight of photons"/ A. Liebert, H. Wabnitz, J. Steinbrink, H. Obrig, M. Möller, R. Macdonald, A. Villringer, and H. Rinneberg // Appl. Opt.– 43(15) – 3037–3047.
8. Elwell C. E. *A practical users guide to near infrared spectroscopy* (1st edition) / Elwell, C. E., Phil M. – Hamatsu Phototonics. – 1995. – KK, London.
9. Jobsis F.F. Noninvasive, Infrared Monitoring of Cerebral and Myocardial Oxygen Sufficiency and Circulatory Parameters. *Science,* 198, 4323, (December 1977). – 1977. – PP. 1264-1267, 0036-8075
10. Wray S. Characterization of the near infrared absorption spectra of cytochrome aa3 and haemoglobin for the non-invasive monitoring of cerebral oxygenation/ Wray, S., Cope, M., Delpy, D. T., Wyatt, J. S., & Reynolds, E. O. R. // *Biochimica et biophysica acta,* 933, (December 1988). – 1988.– PP. 184-192, 0006-3002.
11. Liebert A. Assessment of inflow and washout of indocyanine green in the adult human brain by monitoring of diffuse reflectance at large source-detector separation/ Liebert, A., Sawosz, P., Milej, D., Kacprzak, M., Weigl, W., Botwicz, M., Maczewska, J., Fronczewska, K., Mayzner-Zawadzka, E., Krolicki, L., Maniewski, R. // *Journal of Biomedical Optics,* 16, 4, (April 2011). – 2011. – PP. (046011-1-7), 1560-2281
12. Ellis H. "Anatomy of head injury"/ H. Ellis // Surgery 30. – 2012. – PP. 99–101.
13. Villringer A. "Non-invasive optical spectroscopy and imaging of human brain function"/ Villringer A., Chance B. // Trends Neurosci. 20. –1997.– PP. 435–442–10.1016/S0166-2236(97)01132-6

14. Dehghani H. "Near-infrared spectroscopy of the adult head: effect of scattering and absorbing obstructions in the cerebrospinal fluid layer on light distribution in the tissue"/ Dehghani H., Delpy D. T.– Appl. Opt. 39. –2000 – PP. 4721–4729 10.1364/AO.39.004721
15. Okada E. "Near-infrared light propagation in an adult head model. I. Modeling of low-level scattering in the cerebrospinal fluid layer"/ Okada E., Delpy D. T. – Appl. Opt. 42.–2003.–PP. 2906–2914 10.1364/AO.42.002906
16. Custo A. "Effective scattering coefficient of the cerebral spinal fluid in adult head models for diffuse optical imaging"/ Custo A., Wells W. M., Barnett A. H., Hillman E. M. C., Boas D. A.– Appl. Opt. 45.–2006.– PP. 4747–4755 10.1364/AO.45.004747
17. Del Bianco S., Martelli F., Zaccanti G., "Penetration depth of light re-emitted by a diffusive medium: theoretical and experimental investigation," Phys. Med. Biol. 47, 4131–4144 (2002).10.1088/0031-9155/47/23/301
18. Jacques S. L., "Optical properties of biological tissues: a review," Phys. Med. Biol. 58, 37–61 (2013).10.1088/0031-9155/58/11/R37
19. Cheong W. F., Prahl S. S., Welch A. A., "A review of the optical properties of biological tissues," IEEE J. Quantum Electron. 26, 2166–2185 (1990).10.1109/3.64354
20. Van der Zee P., Essenpreis M., Delpy D. T., "Optical properties of brain tissue," Proc. SPIE 1888 454 (1993).
21. Firbank M., Hiraoka M., Essenpreis M., Delpy D. T., "Measurement of the optical properties of the skull in the wavelength range 650–950 nm," Phys. Med. Biol. 38, 503–510 (1993).10.1088/0031-9155/38/4/002
22. Simpson C. R., Kohl M., Essenpreis M., Cope M., "Near-infrared optical properties of ex vivo human skin and subcutaneous tissues measured using the Monte Carlo inversion technique," Phys. Med. Biol. 43, 2465–2478 (1998).10.1088/0031-9155/43/9/003
23. Yaroslavsky A. N., Schulze P. C., Yaroslavsky I. V., Schober R., Ulrich F., Schwarzmaier H. J., "Optical properties of selected native and coagulated human brain tissues in vitro in the visible and near infrared spectral range," Phys. Med. Biol. 47, 2059–2073 (2002).10.1088/0031-9155/47/12/305
24. Taddeucci A., Martelli F., Barilli M., Ferrari M., Zaccanti G., "Optical properties of brain tissue," J. Biomed. Opt. 1, 117 (1996).10.1117/12.227816
25. Bevilacqua F., Piguet D., Marquet P., Gross J. D., Tromberg B. J., Depeursinge C., "In vivo local determination of tissue optical properties: applications to human brain," Appl. Opt. 38, 4939–4950 (1999).10.1364/AO.38.004939
26. Choi J., Wolf M., Toronov V., Wolf U., Polzonetti C., Hueber D., Safonova L. P., Gupta R., Michalos A., Mantulin W., Gratton E., "Noninvasive determination of the optical properties of adult brain: near-infrared spectroscopy approach," J. Biomed. Opt. 9, 221 (2004).10.1117/1.1628242
27. Comelli D., Bassi A., Pifferi A., Taroni P., Torricelli A., Cubeddu R., Martelli F., Zaccanti G., "In vivo time-resolved reflectance spectroscopy of the human forehead," Appl. Opt. 46, 1717–1725 (2007).10.1364/AO.46.001717
28. Zenkevich O. Finite Element Method in Engineering / O. Zenkevich. - M.: The World, 1975. - 541 p.
29. Taylor R. L. On the completeness of shape functions for finite element analysis / R. L. Taylor // Internat. J. Numer. Methods Eng. — 1972. —V.4. — № 1. — P. 17-22.
30. Wachspress E.I. A rational finite element basis / E.I. Wachspress. — Academic Press. — New York , 1975. — 344 p.
31. Khomchenko A.N. On the probabilistic construction of basic FEM functions / A.N. Khomchenko // Ivano-Frankivs. In-t petrol and gas. - Ivano-Frankivsk, 1982. - 5 p. - Dep. In VINITI on October 21, 1982, No. 5264.
32. Khomchenko A.N. Geometry of Serendip Approximations/A.N. Khomchenko, E.I. Litvinenko, P.I. Guchek // Prikl. Geom. And Ing. graphic arts. - K.: Budivelnik, 1996. - Issue. 59. - PP. 40-42.
33. Popov B.A. Approximation of functions for technical applications / B.A. Popov, G.S. Tesler. - Kiev: Naukova Dumka, 1980. - 352 p.
34. Khomchenko A.N. New approach for building a bazysov serendipity elements / A.N Khomchenko, E.I. Litvinenko, I.A. Astionenko // Geometrical and computer modeling. - 2009 - Vol. 23. - P. 90-95.
35. Wahr, J. A., Tremper, K. K., Samra, S. K., & Delpy, D. T. (1996). Near-infrared spectroscopy: theory and applications. *Journal of Cardiothoracis and Vascular Anesthesia,* 10, 3, (April 1996), pp. (406-418), 1053-0770
36. Germon, T. J., Evans, P. D., Barnett, N. J., Wall, P., Manara, A. R., & Nelson, R. J. (1999). Cerebral near infrared spectroscopy: emitter-detector separation must be increased. *British journal of anaesthesia,* 82, 6, (January 1999), pp. (831-837), 0007-0912
37. Strangman, G., Boas, D. A., & Sutton, J. P. (2002). Non-invasive neuroimaging using nearinfrared light. *Biological psychiatry,* 52, 7, (July 2002), pp. (679-693), 0006-3223
38. Hammoudi, D. (DATE). Meninges, In: *The Brain*, August 1, 2011, Available from: < http://sinoemedicalassociation.org/AP/brainspinalreflexe.pdf>
39. Cope, M. (April 1991). *The application of near infrared spectroscopy to non invasive monitoring of cerebral oxygenation in the newborn infant,* University College London, Retrieved from http://www.medphys.ucl.ac.uk/research/borl/docs/mcope.pdf
40. Madsen, P. L., & Secher, N. H. (1999). Near-infrared oximetry of the brain. *Progress in Neurobiology,* 58, (October 1999), pp. (541-560), 0301-0082
41. Murkin, J. M., & Arango, M. (2009). Near-infrared spectroscopy as an index of brain and tissue oxygenation. *British journal of anaesthesia,* 103, (December 2009), pp. (i3-i13), 1471-6771.
42. Fillerup, D. L., & Mead, J. F. (1967). The lipids of the aging human brain. *Lipids,* 2, 4, (July1967), pp. (295-328), 0024-4201
43. Woodard, H. Q., & White, D. R. (1986). The composition of body tissues. *The British Journal of Radiology,* 59, (June 1986), pp. (1209-1219), 0007-1285

44. Giordano C. Evaluation of Axonal Strain as a Predictor for Mild Traumatic Brain Injuries Using Finite Element Modeling/ C. Giordano, S. Kleiven// Stapp Car Crash Journal. –2014.– Vol. 58 PP.29-61
45. Astionenko I.A. Multiparameter serendipic elements in 2D / I.A. Astionenko, P.I. Guchek, E.I. Litvinenko, A.N. Khomchenko // Bulletin of the Kherson National Technical University. - Kherson, 2010.-№3 (39) - PP.40-47.
46. Segerlind L. Application of the Finite Element Method/L. Segerlind. - Moscow: Mir, 1979. - 392 p.
47. A.N. Khomchenko Construction of basis serendipity spatial elements/A.N. Khomchenko, O.I. Litvinenko, I.O. Astionenko // Applied heom. and engineering graphics /Taurus. state. ahrotehnol. University of. - Vol. 4. – V. 43. - Melitopol: Tavricheskiy State Agrotechnology, 2009. - PP.24-30.
48. Bakker A. Near-Infrared Spectroscopy / A. Bakker, B. Smith, P. Ainslie, K. Smith// Applied Aspects of Ultrasonography in Humans , Prof. Philip Ainslie (Ed.).– InTech ,2012. Available from: http://www.intechopen.com/books/applied-aspects-of-ultrasonography-in-humans/near-infrared-spectroscopy

Рецензент: *д.т.н., проф. Ходаков В.Е.,*
Херсонский национальный технический университет